Iranian Journal of Pharmaceutical Sciences
2026: 22 (1): 501-515
https://journals.sbmu.ac.ir/IJPS

Research Article

OPEN ACCESS

Comparing the Antioxidant Stability of Lipophilic Compounds from Tomato Fruit in Self-Emulsifying Drug Delivery Systems (SEDDS) and in Nano/microemulsion

Annas Binarjo[a] *, Apliana R. Sungkowarini[a], Rizki A.A. Hasibuan[a], Nurkhasanah Mahfudh[b], Verda Farida[a]

[a] *Department of Pharmaceutics and Pharmaceutical Technology, Faculty of Pharmacy, Universitas Ahmad Dahlan, Yogyakarta, Indonesia.*
[b] *Department of Pharmaceutical Chemistry, Faculty of Pharmacy, Universitas Ahmad Dahlan, Yogyakarta, Indonesia.*

Received: November 5, 2025 **Last Revision:** July 24, 2026 **Accepted:** August 5, 2026 **Available online:** November 15, 2026.

Abstract

Lipophilic compounds encounter dissolution problems when administered orally due to their low solubility in gastrointestinal fluids. To improve dissolution performance, several nanocarriers have been implemented, including lipid-based nanocarriers. Presently, self-emulsifying drug delivery systems (SEDDS) and nano/microemulsions have been used to formulate lipophilic antioxidants from tomato (Solanum lycopersicum) fruit and to compare their stability under ambient conditions. The SEDDS is a 1.6% solution of tomato extract in a mixture of Tween 80, Span 80, propylene glycol, and sunflower oil, with mass percentages of 55, 15, 17.5, and 12.5, respectively. The nano/microemulsion was prepared by dispersing the SEDDS in water (1:50). Subsequently, these systems were filled into a colorless, clear glass bottle with a stopper and placed under reflected sunlight during the day and in darkness at night. The antioxidant activity of the formulations was measured by the ABTS method on 0, 1, 3, 5, and 8 days of storage. The order of activity decrease and the rate constant were determined graphically. The results suggested that antioxidant activity decreased following mostly zero-order kinetics, whereas the average R^2 indicated a first-order decline. Three parameters were used for stability comparison, namely zero- and first-order rate constants (k_0 in %/day and k_1 in day^{-1}, respectively) and t_{90} (days), in which those for SEDDS are 1.427+0.061, 0.087+0.005, 1.02+0.10, respectively, while those for nano/microemulsion are 1.231+0.068, 0.048+0.003, 2.61+0.15. It is concluded that the antioxidant activity of tomato extract in nano/microemulsion is more stable in nano/microemulsion than in SEDDS.

Keywords: Antioxidant; Carotenoid; Lipid-based nanocarriers; Nano/microemulsion; SEDDS; Stability; Tomato.

1. Introduction

Tomato (*Solanum lycopersicum)* fruits contain various active substances that exhibit pharmacological activities for maintaining eye health, anticancer properties, neuroprotective activity, and the prevention of degenerative disorders, such as diabetic and cardiovascular disease [1, 2]. Several metabolites in tomatoes responsible for these activities are lutein, zeaxanthin, α-carotene, β-carotene, and lycopene [1 ,3–6], which are lipophilic compounds with poor solubility, resulting in low dissolution and absorption. To overcome this biopharmaceutics issue, the nanocarrier delivery

*** Corresponding Author**:
Annas Binarjo, Department of Pharmaceutics and Pharmaceutical Technology, Faculty of Pharmacy, Universitas Ahmad Dahlan, Yogyakarta, Indonesia. E-mail: annas.binarjo@pharm.uad.ac.id.

Cite this article as: Binarjo A, Sungkowarini A.R., Hasibuan R.A.A., Mahfudh N., Farida V. Comparing the Antioxidant Stability of Lipophilic Compounds from Tomato Fruit in Self-Emulsifying Drug Delivery Systems (SEDDS) and in Nano/microemulsion. Iran. J. Pharm. Sci., 2026, 22 (1): 501- 515.

DOI: https://doi.org/10.22037/ijps.v22i1.50789

This open-access article is distributed under the terms of the Creative Commons Attribution Non Commercial 4.0 License (CC BY-NC 4.0).

system is designed to load the active substances, disperse them in a hydrophilic fluid (the gastrointestinal medium), and facilitate their permeation across lipophilic membranes (the gastrointestinal membrane) [7–9]. Lipid-based formulations, such as self-emulsifying drug delivery systems (SEDDS) and nano/microemulsions (NME), were preferred nanocarriers for lipophilic substances.

SEDDS is a solution of drugs in a mixture of several liquids, including oil (solvent), surfactant, cosurfactant, and cosolvent, in a sufficient concentration, enabling the formation of nanosized droplets once dispersed in water, either producing a kinetically stable nanoemulsion or a thermodynamically stable microemulsion [10]. Therefore, SEDDS is a water-free, preconcentrated oily solution exhibiting significantly less volume than NME. Furthermore, because SEDDS are solutions, unlike NME, they do not undergo several physical instability issues observed in liquid dispersion systems, such as flocculation, coalescence, creaming, and cracking [11]. Moreover, the free-water composition of SEDDS makes them less susceptible to microbial growth [12]. On the other hand, NME offers the possibility of mixing hydrophilic and lipophilic drugs in a single system. The additional convenience is that NME is a ready-to-use liquid dosage form, preferred by persons who have difficulty swallowing, whereas SEDDS is available as solid SEDDS and SEDDS in a capsule [13, 14].

Regarding the chemical stability of the active substance, SEDDS is preferred for delivering ester- or ester-derivative drugs, which are easily degraded in water-containing formulations as emulsions. This hypothesis is derived from previous studies revealing that ester hydrolysis is slower when PEG 400 is added to the aspirin aqueous solution [15]. In another reaction mechanism, the oxidative degradation of ascorbic acid in food was also increased from the dry state to higher water activity [16]. In these systems, chemical stability in a single-phase liquid was investigated, which may differ from that in a multi-phase system, such as an emulsion. For instance, the trend of aspartame degradation in food differed from the two aforementioned studies: the rates of cyclization and amide hydrolysis peaked at a water activity of 0.7. Moreover, the presence of oil in the high-water-activity food mixture also increased the degradation rate [17]. In the present research, the chemical stability of lipophilic tomato extract as an active ingredient was studied to compare the effect of medium, either single-phase or multiple-phase liquid, on the degradation.

The single-phase liquid in the present research is tomato extract SEDDS, a solution of lipophilic material in an oily liquid. The multi-phase liquid consists of a dispersion of the tomato extract SEDDS in water, resulting in surfactant-coated oil droplets containing the tomato extract dispersed within the aqueous phase. The antioxidant activity of both systems was measured as a chemical stability parameter. The decrease in antioxidant activity was calculated to investigate the effect of lipid-based formulation types on drug stability.

2. Materials and Methods

2.1. Materials

Tomatoes were purchased at a local vegetable market in Kotagede, Yogyakarta (Indonesia). The ripe fruit, as identified by the red color, was selected to obtain as much of the carotenoid compound, the lipophilic antioxidant present in tomato. Ethyl acetate, the solvent used to extract carotenoids from tomato, is of analytical grade and produced by Merck (Darmstadt, Germany). Food-grade sunflower oil (SFO) was purchased from El Herbal, Bogor (Indonesia), while Tween 80, Span 80, and propylene glycol (PG) are pharmaceutical-grade products distributed by Bratachem, Yogyakarta (Indonesia). Quercetin and β-carotene standards are of analytical grade from Sigma-Aldrich (China) and supplied by General Labora (Yogyakarta). Purified water was produced by reverse osmosis by the collaboration partner of the Department of Pharmaceutics and Pharmaceutical Technology, Universitas Ahmad Dahlan, Yogyakarta (Indonesia).

2.2. Preparation of Tomato Powder

Fresh, ripe tomatoes were washed thoroughly by running tap water over the fruit to remove potential dirt, including dust and soil, then dried on filter paper. The clean and dry tomatoes were cut into about 1-2 cm cubes using a sharp stainless steel knife before being juiced in a domestic blender (Philips, Indonesia) for about 5 minutes. The water phase of the juice was separated by vacuum filtration, and the solid phase above the filter

This open-access article is distributed under the terms of the Creative Commons Attribution Non Commercial 4.0 License (CC BY-NC 4.0).

was collected and dried at 40 °C for 1 day, producing pomace (dry tomato powder).

2.3. Preparation of Tomato Extract

Ethyl acetate was added to the pomace in a glass beaker, about twice the weight of the powder, followed by stirring for about 1 hour using a hotplate magnetic stirrer (Daihan, Korea) set to 40 °C and 150 rpm. Vacuum filtration was applied to the mixture to remove the undissolved solid phase. Subsequently, the filtrate was evaporated (Maskot Mode RE 1100 V rotary evaporator) to get a concentrated extract, referred to as tomato extract.

2.4. Determination of Carotenoid Content in Tomato Extract

Total carotenoid content was determined according to a previous method with modifications [18]. Briefly, about 10 mg of the tomato extract was weighed precisely (m in mg) using an analytical balance (OHAUS AR 2140, China) and dissolved in ethanol up to 5.0 mL (V) in a volumetric flask. This sample solution was diluted 20-fold (fp) prior to absorbance measurement (Shimadzu UV-1900, Japan) at the maximum wavelength, scanned from 400 to 800 nm. To calculate the carotenoid concentration in the diluted sample solution (Cs, in µg/mL), a calibration curve was constructed by measuring the absorbance of a series of β-carotene solutions in ethanol (5–10 µg/mL) at the same wavelength as the sample. The concentration of carotenoids in the tomato extract (C, in mg/g) was calculated using Equation 1. The parameters and units of the symbols in Equation 4 are provided previously in this paragraph. The unit of concentration is mg β-carotene equivalent/g extract, which is simplified as mg/g.

$$C = \frac{Cs * fp * V}{m} \quad \text{(Eq 1)}$$

2.5. Determination of Flavonoid Content in Tomato Extract

An ethanolic solution of tomato extract at about 20 mg/5 mL, the so-called test sample, was prepared precisely. To 0.5 mL of this solution in a 5 mL volumetric flask, 0.1 mL of 1 M sodium acetate, 0.1 mL of 10% aluminum chloride, and 1.5 mL of ethanol were added sequentially. Purified water was added to the mixture to raise the volume to 5.0 mL. The reaction was allowed to proceed for 20 minutes (optimized) at room temperature before measuring absorbance at the maximum wavelength (443.2 nm). A series of standard samples, quercetin solutions in ethanol, was prepared at concentrations of 50–90 µg/mL. These standard solutions were treated in the same manner as the sample. In the absorbance measurement, each solution was accompanied by a blank solution containing the same components, except aluminum chloride, which was replaced with purified water. The calculated absorbance of each sample is the absorbance reading of the sample minus the absorbance reading of the respective blank solution [19]. The flavonoid concentration in tomato extract (C) is expressed in mg quercetin equivalent/g extract, simplified as mg/g, and calculated using Equation 2, in which Cs, V, and m are the flavonoid concentration in extract solution (tested sample, in µg/mL), volume of tested sample (mL), and the weight of tomato extract (mg), respectively.

$$C = \frac{Cs * V}{m} \quad \text{(Eq 2)}$$

2.6. Construction of Pseudo-ternary Diagrams

Two pseudo-ternary diagrams were prepared as a basis to formulate SEDDS and NME. The first pseudo-ternary diagram consisted of two pure components, namely SFO and PG, and a pseudo-component representing the surfactant mixture (Smix), composed of Tween 80 and Span 80 in a fixed, optimized ratio. The initial system was a mixture of SFO and Smix, as they are completely miscible in all ratios, resulting in a single-phase liquid system. Additionally, to complete the border, the mixture of Smix and a smaller amount of PG, which also produces a single-phase liquid, was also selected as the second starting system. The precise masses of the starting components or pseudo-components were weighed into a pre-weighed vial. The starting systems were stirred using a pre-weighed magnetic bar to ensure homogeneity. The third component, i.e., PG for the first starting system and SFO for the second starting system, was added dropwise using a 20 µl micropipette under constant mild stirring at 350 rpm. Once the systems produced a second phase, the titration was stopped, and the total weight was measured to calculate the mass of

This open-access article is distributed under the terms of the Creative Commons Attribution Non Commercial 4.0 License (CC BY-NC 4.0).

the third component. A similar method and the same basis for initial system selection were also applied in the second pseudo-ternary diagram, composed of SFO, water, and the Smix/PG mixture (referred to as S/C). The initial system consisting of SFO and S/C was titrated using water, mimicking the dispersion of SEDDS. However, to complete the phase diagram, titration of micellar dispersion consisting of S/C and water using SFO was also conducted. A laser pointer (Prolink) was used to distinguish solution, colloidal dispersion, and coarse dispersion.

2.7. Preparation of Blank Self-Emulsifying Drug Delivery System (B-SEDDS)

To confirm the results of pseudo-ternary diagrams, several compositions were prepared (as provided in the supplementary material). Of those compositions, only 3 are shown in **Table 1,** which showed a stable mixture during storage. Each component, as shown in **Table 1,** was weighed for a 10 mL batch volume. Firstly, Tween 80 and Span 80 were transferred to a 20 mL bottle, then stirred at room temperature and 700 rpm for 5 minutes. Subsequently, propylene glycol and oil were added to the surfactant mixture. The stirring was continued for 30 minutes, and the clear solutions, namely F1, F2, and F3, were stored for 2 days to evaluate the physical stability. The clear condition persisted across all formulations, indicating no phase separation. These B-SEDDS were dispersed in water at 1% concentration, and transmittance was measured at 650 nm (Shimadzu UV-1900, Japan). Droplet size was measured using a Malvern Panalytical instrument (The Netherlands) on the formulation with transmittance greater than 90%. The scanning electron microscope (SEM) analysis was also conducted on the dispersion of the selected SEDDS containing tomato extract.

2.8. Preparation of Tomato Extract SEDDS (TE-SEDDS) and Nano/Microemulsion (TE-NME)

About 3 mL of SEDDS was added to the tomato extract in a 10 mL glass bottle. Three levels of tomato extract (10, 20, and 50 mg) were prepared to determine the highest concentration still acceptable to the B-SEDDS. The highest extract concentration that still maintained the solution form was selected for measurement of particle size and polydispersity index. The selected SEDDS is referred to as TE-SEDDS if the droplet size is smaller than 200 nm. TE-NME was prepared by dispersing the selected TE-SEDDS in water at a 1:50 volume ratio.

2.9. Antioxidant Activity of Tomato Extract in Nano/microemulsion

2.9.1. Sample preparation

Blank and tomato extract NME stock were prepared by dispersing 100 µL of B-SEDDS and TE-SEDDS, respectively, in 5 mL of purified water. A series of dilutions using blank NME was performed on the stock emulsion to yield a concentration range of 150-333 mg/L. As a standard, a β-carotene solution in ethanol was prepared at a concentration of 125-185 mg/L.

Table 1. Transmittance, droplet size, and polydispersity index of the B-SEDDS formulation after being dispersed in water at 1%. The data are presented as the mean ± SD of the three replications.

Formulation	Composition (%)				Transmittance (%)	Droplet size (nm)	PI
	Oil	S1	S2	PG			
F1	10	40	20	30	64.37 ± 1.31	Not determined	Not determined
F2	12.5	55	15	17.5	95.49 ± 0.20	125.1 + 1.44	0.568 + 0.003
F3	30	30	22.5	17.5	4.22 ± 0.13	Not determined	Not determined

Note:
1. Oil: sunflower oil, S1: Tween 80 (HLB: 15.0), S2: Span 80 (HLB: 4.3), PG: propylene glycol.
2. The HLBs of the surfactant mixtures in F1, F2, and F3 are 11.4, 12.7, and 10.4, respectively, as calculated using Equation 3, as follows, HLBmix = mass fraction of S1*HLB of S1+mass fraction of S2*HLB of S2 (Eq 3)

This open-access article is distributed under the terms of the Creative Commons Attribution Non Commercial 4.0 License (CC BY-NC 4.0).

2.9.2. ABTS reagent preparation

A solution of ABTS cation radical, so-called ABTS reagent, was prepared by reaction between 0.48 mM 2,2'-azino-bis (3-ethylbenzothiazoline-6-sulfonic acid) solution in water with 0.168 mM potassium persulfate solution in water in equal volume. The reaction was performed for 12-16 hours in dark conditions [20]. This solution is stable for 2 days when kept at room temperature in the dark [21]. In this case, the 0% radical scavenging should be re-measured.

2.9.3. Antioxidant measurement

An equal volume of sample and ABTS reagent was mixed and left to stand in the dark for about 10 minutes to perform radical scavenging by the tomato extract. Subsequently, absorbance at 734 nm was measured to quantify the uncaptured ABTS radical. As a control of 0% radical scavenging, the mixture of ABTS reagent and the medium of each sample was treated in the same way. The percentage of ABTS radical scavenging (denoted as radical scavenging activity, %RSA) of each sample was calculated using Equation 4, in which Ac and As are the absorbance of the control and sample, respectively. The ability of the antioxidant to capture 50% of ABTS, referred to as IC50, was calculated from a linear regression of %RSA as a function of antioxidant concentration [20].

$$\%RSA = \frac{Ac-As}{Ac} x100\% \text{(Eq 4)}$$

2.10. Stability Study of TE-SEDDS and TE-NME

TE-SEDDS and TE-NME in equal amounts of tomato extract were filled into a clear, colorless 10 mL glass bottle. A rubber stopper was set up on the bottle to reduce evaporation. The bottles were then stored in a room illuminated by reflected sunlight during the day and dark at night. The light intensity above the sample was measured using a Samsung handphone light detector (CPUX app by Android). The antioxidant activity of these formulations was tested on 0, 1, 3, 5, and 8 days of storage. For the activity measurement, TE-SEDDS was dispersed using purified water, while the tomato extract NME was directly measured. The curve showing the effect of storage duration on %RSA was analyzed graphically to determine the kinetic order and the rate constant of activity decline for each replicate, hereafter referred to as "an individual subset". Based on these data, stability parameters were outlined for stability comparison, including the storage time at which the activity decreases to 90% of the initial value (t90), calculated using Equations 5, 6, and 7 depending on the declining order. The stability parameters were statistically analyzed using an independent sample t-test (SPSS 17).

$t_{90} = 0.1*RSA_0/k_0$ (Eq. 5)

$t_{90} = 0.105/k_1$ (Eq. 6)

$t_{90} = 0.111/(k_2*RSA_0)$ (Eq. 7)

3. Results and Discussion

3.1. Preparation and Chemical Determination of Tomato Extract

As a preformulation study to select a lipid-based formulation for lipophilic tomato extract, chemical stability studies of SEEDS and NME were conducted, starting with the preparation of the tomato extract. Tomato fruit contains a large amount of water, which needs to be removed before extraction. Five steps of extraction, namely juicing the tomatoes, vacuum filtering the juice, drying the solid residue (pomace), macerating the residue, and concentrating the macerate, produced a dark red, sticky extract. The yield of tomato powder (dry pomace) calculated from fresh tomato fruit was 1.4%, while the yield of concentrated extract based on tomato powder was 2.6%. Since the extraction solvent is ethyl acetate, the concentrated extract is lipophilic. The carotenoid and flavonoid content, as a targeted group of antioxidants available in tomato lipophilic extract, was determined by spectroscopy using β-carotene and quercetin as standards for calibration curve construction. The data are shown in **Figure 1**.

In previous studies, the total carotenoid concentration (as β-carotene and lycopene) in tomato peels was about 0.85 mg/g dry solids [22]. Combining this previous data with the carotenoid concentration (about 11.7 mg/g) and the extract yield (2.6%) in the present study, it is suggested that the extraction recovery is approximately 36%. The carotenoid concentration in the extract and the carotenoid recovery of the extraction process in the present study are higher than those obtained with supercritical fluid carbon dioxide extraction and functionalized oil [22, 23]. However, due to the toxicity issue, such previously used extraction solvents are likely preferred, although ethyl acetate is included in Class III, the lowest-toxicity organic solvent, together with acetic acid, acetone, and ethanol [24].

This open-access article is distributed under the terms of the Creative Commons Attribution Non Commercial 4.0 License (CC BY-NC 4.0).

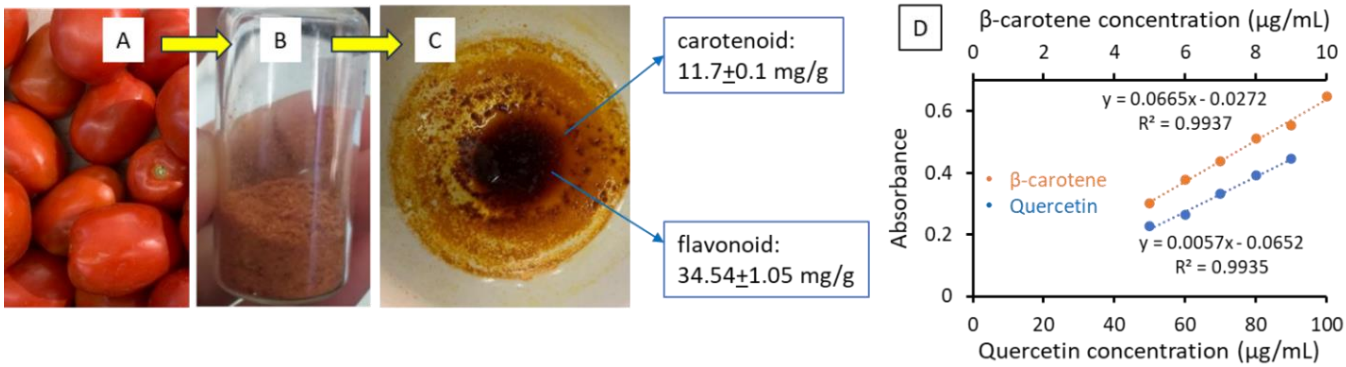


Figure 1. Visual appearance of fresh tomato fruit (A), dry tomato powder (B), concentrated tomato extract (C), and calibration curve for carotenoid and flavonoid quantification in concentrated tomato extract (D). The absorbance of sample and standard solutions was measured at the maximum wavelengths of 449.9 and 443.2 nm for carotenoid (without any reagent) and flavonoid (with $AlCl_3$) determination, respectively. The total carotenoid and total flavonoid concentrations in the extract are provided as the mean ± SD of 3 replications.

Regarding flavonoids, tomato contains both glycosidic and non-glycosidic flavonoids in almost equal amounts, mostly rutin and naringenin chalcone [25]. Using ethyl acetate as an extractor solvent, only the non-glycosidic flavonoids are brought into the concentrated extract. The extraction yield of 2.6% concerning dry pomace, the recovery of non-glycosidic flavonoids in the present research is about 12%, much lower than the carotenoid recovery. Ethyl acetate, a lipophilic solvent, was likely saturated with the semipolar flavonoids in the extraction process.

3.2. Preparation and Characterization of Blank Self-Emulsifying Drug Delivery System (B-SEDDS)

B-SEDDS consists of four single components, namely SFO, Tween 80, Span 80, and propylene glycol. To determine the liquid-phase number for these 4 components when mixed in various proportions, a phase diagram was constructed. Two surfactants were kept at a constant ratio, producing a pseudo-component, which allowed the drawing of a pseudo-ternary diagram as shown in **Figure 2**.

Figure 2 suggests that, while PG only accepts the Smix up to about 60%, SFO and Smix are completely miscible, forming a single liquid phase that is used as the initial system. Titrating this system with PG yields a three-component system that initiates separation at a specific PG concentration. The initial system consists of more Smix, keeping the state in solution in more titrated PG. The B-SEDDS composition in the present research is located in this more Smix area. Increasing the SFO fraction to 30% at a constant PG (17.5%) is sufficient to maintain the solution state when the Tween 80 and Span 80 ratio in Smix is shifted; however, this system fails to disperse colloidal particles, as discussed in the following paragraph.

The pseudo-ternary diagram of **Figure 2** was expanded by varying the ratios of surfactant (Tween 80), cosurfactant (Span 80), cosolvent (propylene glycol), and oil (sunflower oil), as shown in **Table 1**. These formulations remained stable as solutions during storage for more than 2 days (they were not evaluated beyond this period), whereas other compositions exhibited liquid-phase separation (see supplementary file). Only F2 exhibited transmittance greater than 90% upon dispersion in water. The high transmittance at 650 nm indicates that the droplet size is mostly in the colloidal range, identifying that the system is a nanoemulsion or microemulsion. Therefore, only F2 potentially has an average droplet size less than 500 nm, a requirement for NME [26], as confirmed by particle size analysis (**Table 1**).

This open-access article is distributed under the terms of the Creative Commons Attribution Non Commercial 4.0 License (CC BY-NC 4.0).

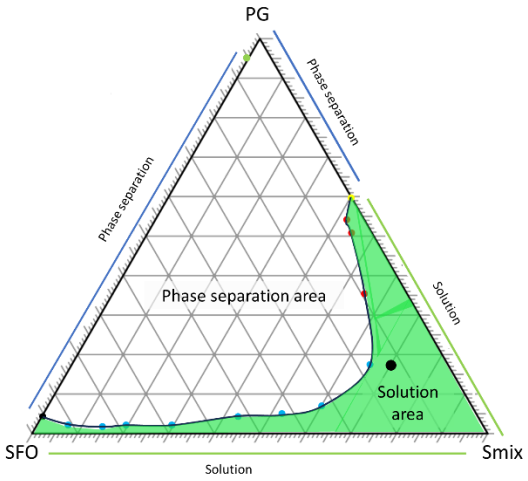


Figure 2. Pseudo-ternary diagram to assist in selecting the fractions of sunflower oil (SFO), Tween 80-Span 80 mixture at 55:15, respectively (Smix), and propylene glycol (PG) for B-SEDDS preparation. The blue solid circles are the border between separated and unseparated zones when the SFO-Smix initial systems were titrated using PG; whereas the red ones, which are also the border, were identified by SFO titration. The black solid circle is the composition of B-SEDDS of F2 in **Table 1**, i.e., 12.5%, 70%, and 17.5% for SFO, Smix, and PG, respectively.

The F2 comprises oil, a surfactant mixture, and a cosolvent at a mass ratio of 1:5.6:1.4, resulting in a surfactant-to-oil ratio much higher than that of F3 (1:1.75). It is reasoned that the droplet size of F3, predicted from the transmittance, is above the size of the colloidal dispersion internal phase. A higher surfactant-to-oil ratio increases the likelihood that SEDDS will form a larger oil-to-water interface, resulting in a smaller droplet size [27]. The surfactant-to-oil ratio in F1 is slightly higher than in F2, namely 6:1, but the proportion of surfactant (Tween 80) and cosurfactant (Span 80) results in a lower hydrophilic-lipophilic balance (HLB) than in F2. The required hydrophilic-lipophilic balance (HLB) of sunflower oil has not yet been established. However, another vegetable oil, namely virgin coconut oil (VCO), requires an HLB of approximately 14 to form a stable NME [28]. Since sunflower oil is similar in composition to VCO, namely more than 97% is triglyceride [29], we assume that the RHLB is close to 14. Based on the HLB-RHLB conformity theory on emulsion stability [30], the F2 tends to be more stable than F1 since the HLB of the surfactant mixture in F2 is 13.2, while that in F1 is 6.9. The dispersion process of a solution containing SFO and S/C (a mixture of Smix and PG in a constant ratio) with water, as exemplified in the previous discussion of NME composition, can be illustrated by expanding the percentages of S/C, SFO, and water, producing a pseudo-ternary diagram. The pseudo-ternary diagram is shown in **Figure 3.**

Figure 3 suggests that the mixture of oil, surfactant, cosolvent, and water exhibits at least 4 phases: liquid-liquid colloidal dispersion (blue and green areas), gel colloidal dispersion (purple area), cream (yellow area), and coarse liquid-liquid dispersion (emulsion). The target of B-SEDDS dispersion is the green area by water addition, which is likely different, particularly in terms of area size, from the present phase diagram step of preparation, i.e., SFO titration. Due to mild stirring, SFO drops were difficult to disperse into the S/C-water mixture to form a colloidal liquid-liquid dispersion, resulting in a low area (green), whereas dispersing B-SEDDS with water easily forms NME.

3.3. Preparation and Characterization of Tomato Extract SEDDS (TE-SEDDS)

Simply introducing tomato extract to B-SEDDS, followed by mild magnetic bar stirring, yielded a clear solution at 1.6% concentration, referred to as TE-SEDDS. The lipophilic nature of tomato extract is compatible with B-SEDDS, in line with the "like dissolves like" principle [31]. Dispersing TE-SEDDS in water produced a clear nanoemulsion showing a droplet size and polydispersity index that are not significantly different from B-SEDDS dispersion, as shown in **Figure 4**.

This open-access article is distributed under the terms of the Creative Commons Attribution Non Commercial 4.0 License (CC BY-NC 4.0).

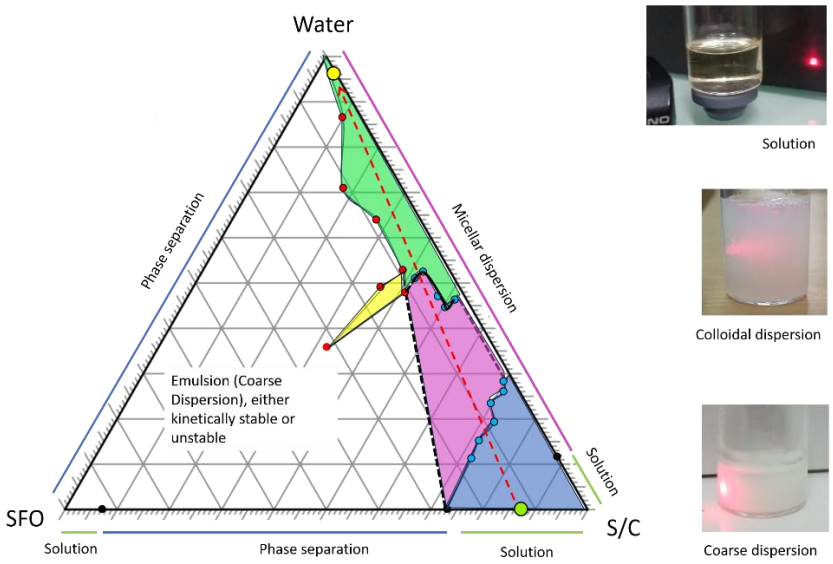


Figure 3. A pseudo-ternary diagram consists of sunflower oil (SFO), a mixture containing Smix and PG at a 4:1 (S/C) ratio, and water. The blue solid circle shows the boundary composition obtained from water titration of the SFO and S/C mixture as the initial system, while the red solid circles were identified by SFO titration. The boundary of two components (or pseudo-components) is shown as black solid circles. Ordered area from the bottom, i.e., the blue, purple, yellow, and green show high viscosity colloidal dispersion, gel-like, cream-like, and O/W nano/microemulsion, respectively. The dashed black line is the imaginary border, while the dashed red arrow shows B-SEDDS (green circle) imaginary titration using water, producing the present NME (yellow circle). Interaction of a low-intensity laser beam pointer with solution, colloidal dispersion (including nano/microemulsion), and coarse dispersion (such as emulsion) is depicted on the right-hand side.

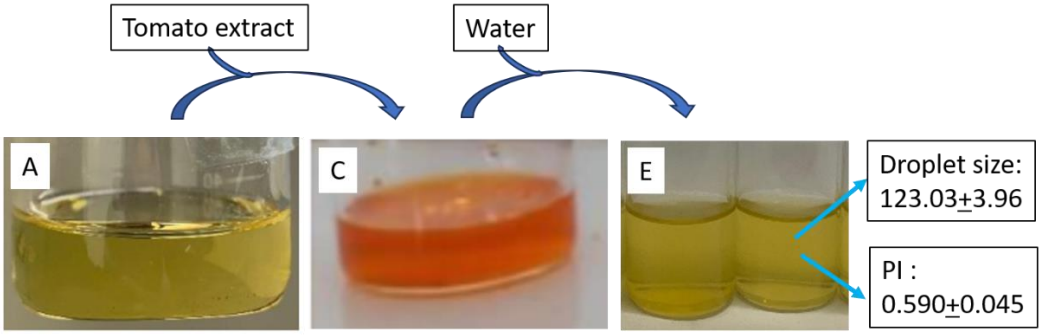


Figure 4. Physical appearance of B-SEDDS (A), TE-SEDDS (C), and TE-SEDDS dispersion in water (NME, E). The droplet size and polydispersity index (PI) are provided as mean ± SD from three replications.

The droplet size meets the size requirement for an NME, while the polydispersity index of more than 0.4 indicates that the system is a polydisperse colloid [32], in line with the size distribution graph showing 2 peaks (**Figure 5**). The high variation in the size of the internal phase is also evident in an SEM image showing two types of single units of the internal phase: a single droplet and a flocculate, an aggregate of droplets. The polydispersity index is the relative standard deviation (RSD, coefficient of variation, CV) of the average particle/droplet size in a bulk measured using PSA during a run. A higher PI indicates that the emulsion droplets span a wide size range. However, it does not mean that the system is a heterogeneous colloidal dispersion. Usually, NME is a homogeneous system, either monodisperse or polydisperse, since the droplet shape in a bulk of emulsion is the same, i.e., spherical, as captured using Scanning Electron Microscope (SEM) [33, 34].

This open-access article is distributed under the terms of the Creative Commons Attribution Non Commercial 4.0 License (CC BY-NC 4.0).

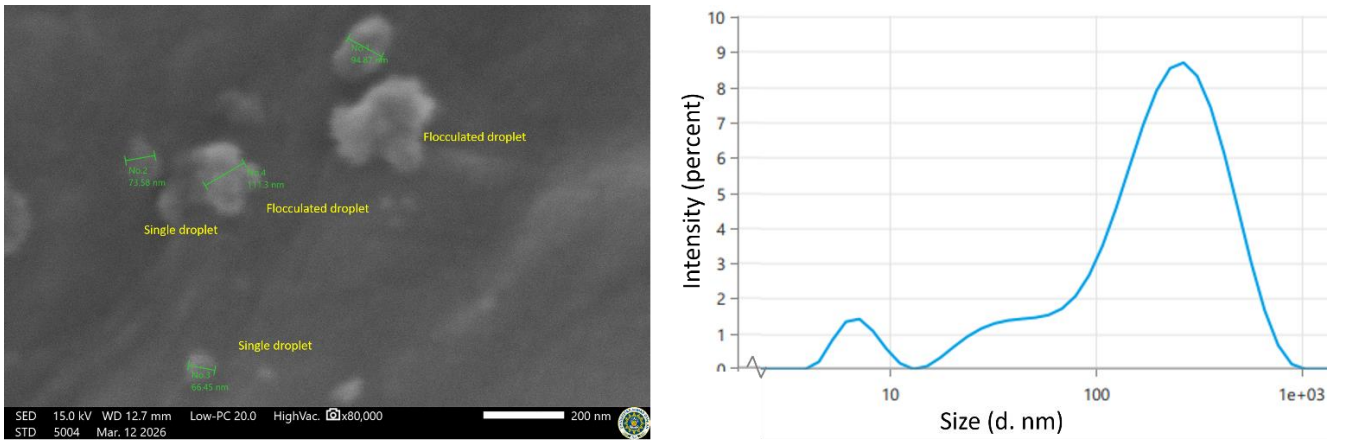


Figure 5. A typical SEM image (left) and size distribution (right) of nano/microemulsion produced by TE-SEDDS dispersion in water 1:50.

3.4. Antioxidant Activity of Tomato Extract

Antioxidant activity of the lipophilic tomato extract was measured as an NME since this material is practically insoluble in water. Dissolving this material in a water-miscible solvent, such as ethanol or acetone, at a very dilute concentration produced a water-partially miscible solution, showing two liquid phases in separate layers. The NME resulting from TE-SEDDS dispersion in water was diluted using B-SEDDS dispersion to prepare tomato extract NME in various concentrations. Reacting these colloidal dispersions with ABTS radical reduced the bluish green (or green blue/turquoise) color of the radical to a certain level, proportional to the tomato extract concentration, as shown in **Figure 6**.

Figure 6 shows that β-carotene is more effective at quenching the ABTS radical than tomato extract, a common issue because the extract contains various materials, including both active and inactive substances. Carotenoids are the main lipophilic antioxidant compounds in tomato, comprising at least five non-hydroxy carotenoids, namely β-carotene, lycopene, phytoene, phytofluene, and α-carotene (listed from highest to lowest). In contrast, the hydroxy carotenoids (lutein and zeaxanthin) are less abundant than α-carotene [35]. Additionally, in the present tomato extract, antioxidant activity was supported by other substances, particularly flavonoids, which are present at higher concentrations than carotenoids (**Figure 1**). The antioxidant activity of flavonoids and other polyphenol substances has been reviewed previously [36]. In the present research, the antioxidant activity of compounds other than carotenoids was also demonstrated, as described below. In 300 mg/L of tomato extract (the 4th data point of tomato extract antioxidant activity measurement), about 3.5 mg/L of carotenoid is available, as calculated by multiplying the extract concentration in the antioxidant-tested solution by the carotenoid content in the extract. However, the antioxidant activity of this solution is higher than that of the 125 mg/L β-carotene solution, the first data point in the measurement of β-carotene antioxidant activity.

To compare the antioxidant strength with that of other studies, which are often reported at different concentrations, the concentration producing 50% radical scavenging (IC50) is calculated from the linear curve of concentration vs % scavenging, or log concentration vs % scavenging if the curve is exponential [37, 38]. In the present research, the IC50 was calculated by forward forecasting of concentration vs RSA (**Figure 6**), and the results are listed in **Table 2**.

Table 2. IC50 of tomato extract and β-carotene, as a standard reference substance, was measured using the ABTS method. The data are presented as the mean ± SD from 4 replicates. Relative antioxidant activity was calculated as a ratio of the IC50 of the reference substance/IC50 of the substance of interest.

Antioxidant	IC50 (mg/L)	Relative antioxidant activity (%)
Tomato extract	544.5 + 9.4	43
B-carotene	232.4 + 1.8	100

This open-access article is distributed under the terms of the Creative Commons Attribution Non Commercial 4.0 License (CC BY-NC 4.0).

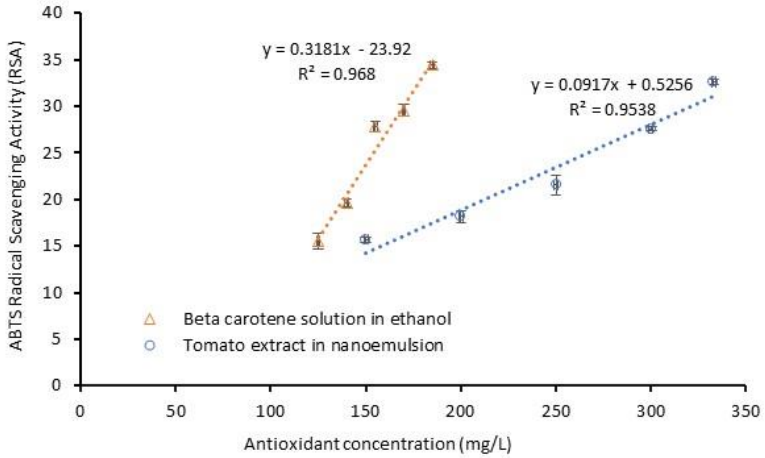


Figure 6. Correlation between the concentration of antioxidant materials, including β-carotene and tomato extract, and the capability to capture ABTS cation radical as the basis of antioxidant activity calculation.

Relative antioxidant activity exhibited in **Table 2** is better than IC50 in comparing antioxidant strength if the reference substance is the same. However, when measuring antioxidant activity using different references, IC50 is the second-line measure that can be compared. Based on the IC50 in **Table 2**, the antioxidant activity of the lipophilic extract in the present research is higher than that of the dispersed and dissolved material of tomato juice, which showed an IC50 of 1.9 g/L, which is likely due to the large number of undissolved carbohydrates (fiber) in the juice [20]. When the undissolved fraction is removed, as in extracts, the antioxidant activity of water and acetone extracts, which are more hydrophilic, is higher than that of the ethyl acetate extract [39], as observed in the present research. The high ascorbic acid content in the hydrophilic extract is responsible for its antioxidant activity. However, lipophilic antioxidants cannot be underestimated in radical protection; they work in the lipid phase, such as the cell membrane. By adding hydrophilic antioxidants, such as flavonoids (particularly glycosidic ones) and vitamin C, a synergistic antioxidant action is delivered, especially at higher ratios than lipophilic antioxidants [40].

3.5. Stability of Antioxidant Activity of the Tomato Extract in SEDDS and NME Preparation

The position of the tomato extract antioxidant in the microregion of SEDDS preparation and NME is different. In SEDDS, the antioxidant molecules are distributed homogeneously throughout the system, since it is a liquid single-phase (solution), whereas in NME, the extract is distributed between the oil droplet phase and the aqueous medium phase at different levels. The extract concentration in the oil droplet is higher than that in the disperse medium due to the lipophilic nature of the extract. This affects the antioxidant stability compared in the present research, starting with the determination of the kinetic order of activity decrease using the graphical method. The results are shown in **Figure 7** and **Table 3**.

Table 3. Determination of the kinetics order of decrease in antioxidant activity.

Formulation	Number of individual subsets showing specific order			Average R^2		
	zero	first	second	zero	first	second
SEDDS	0	1	3	0.9358	0.9564	0.9629
NME	4	0	0	0.8736	0.8539	0.8303
Both	4*	1	3	0.9047	0.9051**	0.8966

*Most declines follow zero-order kinetics
** The highest R^2 average is the first-order model

This open-access article is distributed under the terms of the Creative Commons Attribution Non Commercial 4.0 License (CC BY-NC 4.0).

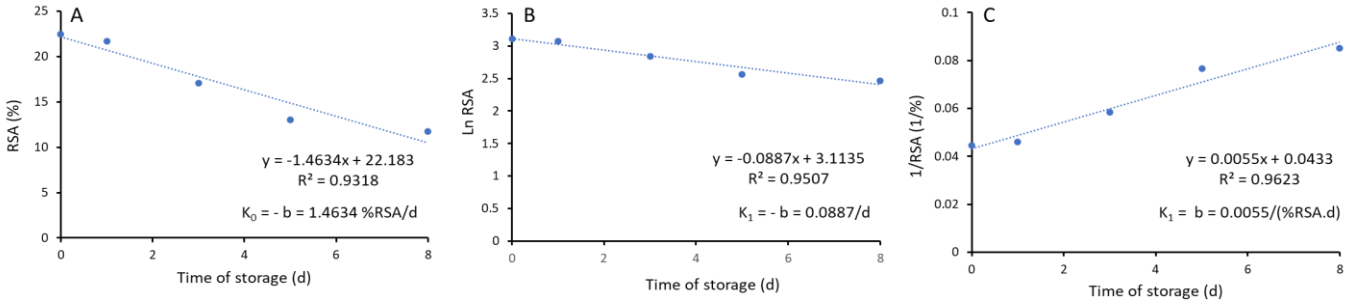


Figure 7. Description of the graphical method for the determination of the kinetic order. The example is the first replicate of SEDDS preparation. The correlation between time of storage (t, x-axis) and radical scavenging activity (RSA, y-axis) was plotted in three linear models, i.e, without transformation (RSA vs t, representing zero order, Figure 4. A), with y-axis transformation by natural logarithmic (ln RSA vs t, representing first order, Figure 4. B), and with y-axis transformation by inversion (1/RSA vs t, representing second order, Figure 4. C). The closer R^2 to 1 means the model is the best-fitted one. The example demonstrates that the order of decrease in antioxidant activity follows second-order kinetics (R^2 = 0.9623). The constant rate of decline of each order is also displayed.

The best approach to assess the stability of the antioxidant activity of tomato extract in SEDDS and NME preparations is to compare the rate constant (k) of decrease. This method only works if the kinetic order of decline is the same or assumed to be the same. As shown in Table 3, the kinetic order of decrease varies in all orders. In comparing the k, we thought that all decreases follow the zero-order, since most of the decline follows this order (4 of 8 individual subsets), and the first-order, since the highest average R^2 is in this order. An alternative approach was used by comparing the time needed to decrease the antioxidant activity to 90% (t_{90}, the most accepted shelf life of products), calculated using the formula according to their respective order, as in equations 5, 6, and 7 for zero-, first-, and second-order, respectively [41]. In the formula, RSA_0 is the initial (before storage) antioxidant activity, while k_0, k_1, and k_2 are the constant rates of degradation of zero-order, first-order, and second-order, respectively. The results are exhibited in **Table 4**.

All stability parameters in **Table 4** suggest that the antioxidant activity decline of tomato extract in SEDDS preparation is faster than that in NME by 1.2, 1.8, and 2.6-fold, based on k_0, k_1, and t_{90}, respectively. This is in line with the generally accepted rule that encapsulation increases stability by protecting the drug from environmental factors, including chemical (pH, oxygen, enzyme) and physical (light, humidity) factors [42, 43]. In a previous study, it was proven that the stability of drugs in a lipid nanocarrier is higher than in solution [44]. In the present research, tomato extract was prepared in two systems: a solution in SEDDS and in NME, which were stored under normal light in a clear, color-free bottle. Ethyl acetate, currently used as an extraction solvent, determines the lipophilic properties of the tomato extract, leading to the accumulation of active substances in the cores of nanodroplets during NME preparation. The schematic representation of these two systems is depicted in **Figure 8**.

Table 4. Stability parameters to compare the decline of antioxidant activity during storage for 8 days at ambient temperature, RH, and light. The data are the mean + SD of four replicates.

Formulation	k_0 (%RSA/day)	k_1 (1/d)	t_{90} (d)*
SEDDS	1.427 + 0.061	0.087 + 0.005	1.02 + 0.10**
NME	1.231 + 0.068	0.048 + 0.003	2.61 + 0.15***
sign. (p)****	0.005	0.000	0.000

* The individual subsets are calculated independently using the respective order
** Three individual subsets follow second-order kinetics, and one individual subset follows first-order.
***All individual subsets follow zero-order kinetics
****Based on an independent-samples t-test between SEDDS and NME

This open-access article is distributed under the terms of the Creative Commons Attribution Non Commercial 4.0 License (CC BY-NC 4.0).

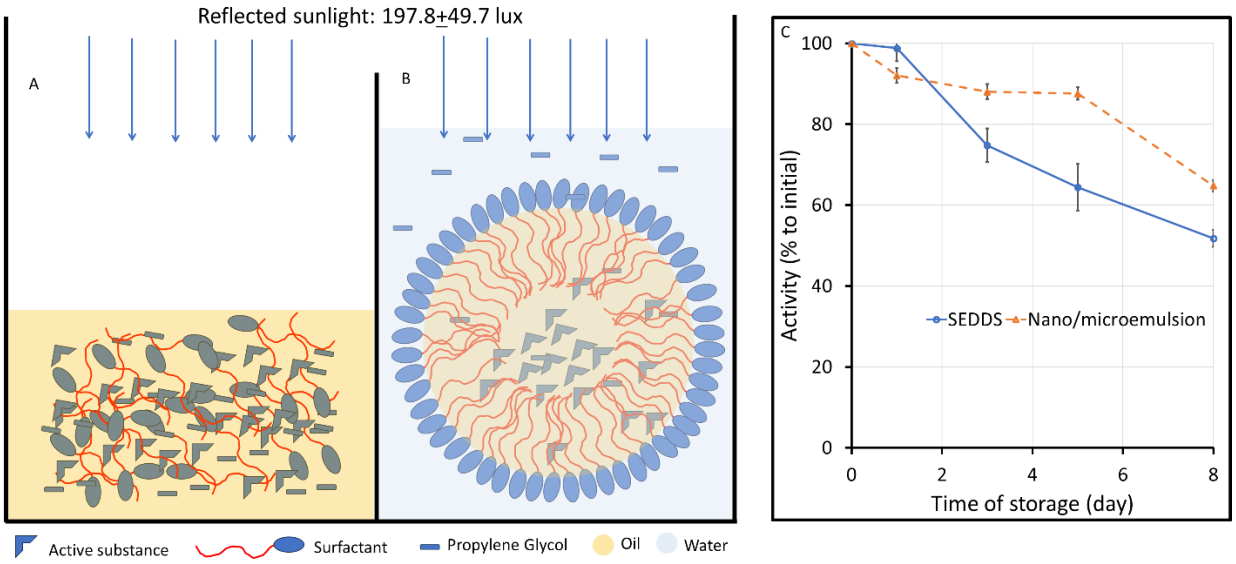


Figure 8. Visualization of SEDDS, a solution containing active substance (tomato extract), surfactants (Tween 80 and Span 80), cosolvent (propylene glycol), and oil (sunflower oil, yellow background) (A). A droplet of nano/microemulsion dispersed in water (light blue background) (B). A surfactant consists of a lipophilic tail (red) and a hydrophilic head (blue), forming a droplet that stabilizes the oil phase where the active substance is located. Activity decrease is shown by the effect of storage time on the percentage of RSA at the specified time relative to the initial (C).

Figure 8 suggests that, in an NME system, drugs are encapsulated within lipophilic cores. The surface layer of the lipophilic core is composed of the surfactant's hydrophilic part, serving as a coating that protects the active substances in the droplet core from light. This protection significantly increases stability, as the active substance is degraded primarily by oxidation [45], which can be catalyzed by light [46]. Moreover, the oxygen concentration surrounding the antioxidant in SEDDS is higher than in NME, since the solubility of oxygen in oil, equivalent to SEDDS, is higher than that in water [47], the medium of nanosized droplets. Therefore, in NME, in addition to light protection provided by the surfactant umbrella, the active substance is also protected by water from oxygen attack. Additionally, when technical-grade Tween 80 and Span 80 are used as surfactants in NME preparation, the peroxide impurity from the surfactants [48] partitions into water, reducing the concentration around the drugs. This impurity is a potent catalyst for oxidation [49], which should be kept away from the easily oxidized drugs. Even though these three mechanisms contribute to the higher stability of tomato extract in NME, they may not work for active substances susceptible to hydrolysis due to the water available in NME. This result complements the previous method for enhancing carotenoid stability using chitosan nanoparticles [50].

4. Conclusion

The lipid-based formulations of lipophilic antioxidant compounds from tomato, represented by ethyl acetate tomato extract, have been formulated in two preparations with a similar ratio of non-water components: SEDDS and nano/microemulsion. An activity stability study of these preparations, performed by measuring radical scavenging activity against ABTS+• during storage under intermittent reflected sunlight at room temperature, revealed that the droplet nanocarrier, the internal phase of the nano/microemulsion, protects the drug from light, a catalyst of oxidation, thereby enhancing stability. The dispersed medium of a nano/microemulsion, which contains water with a small amount of propylene glycol, is also likely to support stability improvement by reducing the exposure of the antioxidant compound to atmospheric oxygen. This data supports the generally accepted rule that drugs in a nanocarrier exhibit greater stability than in solution.

This open-access article is distributed under the terms of the Creative Commons Attribution Non Commercial 4.0 License (CC BY-NC 4.0).

Acknowledgment

The authors would like to thank Lembaga Penelitian dan Pengabdian Masyarakat (LPPM) Universitas Ahmad Dahlan Yogyakarta, which supports the funding by a grant numbered PD-035/SP3/LPPM-UAD/XII/2023.

Conflict of interest

There is no conflict of interest to be declared.

Data availability

All data are presented in the article, specifically as mean values and standard deviations. Raw data are stored in AB's private storage.

Authors Contributions

A.B., V.F., and N.M. conceptualized the study; A.B., A.R.S., and R.A.A.H. contributed to methodology and formal analysis; A.B., A.R.S., and R.A.A.H. contributed to investigation and data curation; A.B. and V.F. contributed to writing the original draft; all authors contributed to writing, review, & editing.

Authors Orcid numbers:

Annas Binarjo: 0000-0001-8956-3261
Apliana R. Sungkowarini: 0009-0004-2836-4989
Rizki A.A. Hasibuan: 0009-0001-3811-3399
Nurkhasanah Mahfudh: 0000-0001-6156-4318
Verda Farida: 0000-0003-1448-2111

Funding

Lembaga Penelitian dan Pengabdian Masyarakat (LPPM) Universitas Ahmad Dahlan Yogyakarta.

Using artificial intelligence chatbots

No artificial intelligence was used in the preparation of this article.

References

1. Wu Y, et al. Enrichment of health-promoting lutein and zeaxanthin in tomato fruit through metabolic engineering. *Synth. Syst. Biotechnol.* (2022)7(4):1159–1166.
2. Collins EJ, Bowyer C, Tsouza A, Chopra M. Tomatoes: An Extensive Review of the Associated Health Impacts of Tomatoes and Factors That Can Affect Their Cultivation. Biology. (2022) 11 (2): 239.
3. Middha P, Weinstein SJ, Männistö S, Albanes D, Mondul AM. β-Carotene Supplementation and Lung Cancer Incidence in the Alpha-Tocopherol, Beta-Carotene Cancer Prevention Study: The Role of Tar and Nicotine. Nicotine Tob. Res. (2018) 21 (8): 1045–1050.
4. Huang Y, Chen H, Su Y, Liu H, Hu J, Hong K. Increased blood alpha-carotene, all-trans-Beta-carotene and lycopene levels are associated with beneficial changes in heart rate variability: a CVD-stratified analysis in an adult population-based study. Nutr. J. (2021) 20 (1): 43.
5. Park H-A, Hayden MM, Bannerman S, Jansen J, Crowe-White KM. Anti-Apoptotic Effects of Carotenoids in Neurodegeneration. Molecules. (2020) 25 (15): 3453.
6. Zhu R, et al. Lycopene in protection against obesity and diabetes: A mechanistic review. Pharmacol. Res. (2020) 159 (Sept):104966.
7. Feng W, et al. Natural sesame oil is superior to pre-digested lipid formulations and purified triglycerides in promoting the intestinal lymphatic transport and systemic bioavailability of cannabidiol. Eur. J. Pharm. Biopharm. (2021) 62 (May): 43–49.
8. Dahan A, Hoffman A. The effect of different lipid based formulations on the oral absorption of lipophilic drugs: The ability of in vitro lipolysis and consecutive ex vivo intestinal permeability data to predict in vivo bioavailability in rats. Eur. J. Pharm. Biopharm. (2007) 67 (1): 96–105.
9. Feng W, et al. Inclusion of Medium-Chain Triglyceride in Lipid-Based Formulation of Cannabidiol Facilitates Micellar Solubilization In Vitro, but In Vivo Performance Remains Superior with Pure Sesame Oil Vehicle. Pharmaceutics. (2021) 13 (9): 1349.
10. Buya AB, Beloqui A, Memvanga PB, Préat V. Self-Nano-Emulsifying Drug-Delivery Systems: From the Development to the Current Applications and Challenges in Oral Drug Delivery. Pharmaceutics. (2020) 12 (12): 1194.
11. Thakur R, Sharma A, Verma P, Devi A. A Review on Pharmaceutical Emulsion. Asian J. Pharm. Res. Dev. (2023) 11 (3): 168–172.
12. Peleg M, Corradini MG, Normand MD. On Modeling the Effect of Water Activity on Microbial Growth and Mortality Kinetics. In: Gutiérrez-López GF, Alamilla-Beltrán L, del Pilar Buera M, et al., (Eds). Water Stress Biol Chem Pharm Food Syst [Internet]. New York, NY: Springer; 2015 [cited 2025 Sept 29]. p. 263–278. Available from: https://doi.org/10.1007/978-1-4939-2578-0_19.
13. Musakhanian J, Ellis I, Dave M. Transforming Liquid SEDDS into Solid Oral Dosage Forms [Internet]. 2022 [cited 2025 Sept 29]. Available from: https://www.americanpharmaceuticalreview.com/Featured-Articles/584546-Transforming-Liquid-SEDDS-into-Solid-Oral-Dosage-Forms/.
14. Gursoy RN, Benita S. Self-emulsifying drug delivery systems (SEDDS) for improved oral delivery of lipophilic drugs. Biomed. Pharmacother. (2004) 58 (3): 173–182.
15. Bakar SK, Niazi S. Stability of aspirin in different media. J. Pharm. Sci. 1983;72(9):1024–1026.

This open-access article is distributed under the terms of the Creative Commons Attribution Non Commercial 4.0 License (CC BY-NC 4.0).

16. Lee SH, Labuza TP. Destruction of Ascorbic Acid as a Function of Water Activity. J Food Sci. (1975) 40 (2): 370–373.
17. Bell LN, Labuza TP. Aspartame Degradation as a Function of "Water Activity." In: Levine H, Slade L, (Eds). Water Relatsh Foods Adv 1980s Trends 1990s [Internet]. Boston, MA: Springer US; 1991 [cited 2025 Oct 1]. p. 337–349. Available from: https://doi.org/10.1007/978-1-4899-0664-9_19.
18. Hagos M, Redi-Abshiro M, Chandravanshi BS, Yaya EE. Development of Analytical Methods for Determination of β-Carotene in Pumpkin (Cucurbita maxima) Flesh, Peel, and Seed Powder Samples. *Int. J. Anal. Chem.* (2022) 2022: 9363692.
19. Direktorat Jenderal Farmasi dan Alat Kesehatan. Farmakope Herbal Indonesia Edisi II [Internet]. Jakarta: Kementrian Kesehatan Republik Indonesia; 2017 [cited 2025 Oct 17]. Available from: https://farmalkes.kemkes.go.id/2020/08/farmakope-herbal-indonesia-edisi-ii-tahun-2017-3/.
20. Binarjo A, Afifaturahma I, Cahyani E, Praty P. Wound healing activity of cream formulation containing tomato juice in guinea-pig: Development of measurement analysis and its application. J. Phytomedicine Ther. (2025) 24 (1): 2020–2040.
21. Re R, Pellegrini N, Proteggente A, Pannala A, Yang M, Rice-Evans C. Antioxidant activity applying an improved ABTS radical cation decolorization assay. Free. Radic. Biol. Med. (1999) 26 (9): 1231–1237.
22. Colucci Cante R, Gallo M, Varriale L, Garella I, Nigro R. Recovery of Carotenoids from Tomato Pomace Using a Hydrofluorocarbon Solvent in Sub-Critical Conditions. Appl. Sci. (2022) 12 (6): 2822.
23. Vági E, Simándi B, Vásárhelyiné KP, Daood H, Kéry Á, Doleschall F, Nagy B. Supercritical carbon dioxide extraction of carotenoids, tocopherols and sitosterols from industrial tomato by-products. J. Supercrit. Fluids. (2007) 40 (2): 218–226.
24. European Medicines Agency (EMA). ICH Q3C (R9) Residual solvents - Scientific guideline [Internet]. 2024 [cited 2025 Oct 2]. Available from: https://www.ema.europa.eu/en/ich-q3c-r9-residual-solvents-scientific-guideline.
25. Zhou L, et al. Increasing flavonoid contents of tomato fruits through disruption of the SlSPL-CNR, a suppressor of SlMYB12 transcription activity. Plant Biotechnol. J. (2024) 22 (2): 290–292.
26. McClements DJ. Nanoemulsions versus microemulsions: terminology, differences, and similarities. Soft Matter. (2012) 8 (6): 1719–1729.
27. Zeighami A, Kargozarfard Z, Khiabani NP, Ayatollahi S. Salt-acid-surfactant synergistic effects on interfacial characteristics of water/oil systems: A molecular dynamics simulation study. J. Mol. Liq. (2024) 396: 123996.
28. Setyopratiwi A, Hanifah HTU. Formulasi dan Stabilitas Mikroemulsi Minyak dalam Air dengan Virgin Coconut Oil (VCO) Sebagai Fase Minyak Menggunakan Metode Emulsifikasi. Prosiding Seminar Nasional Kimia. (2022) 1: 108–123.
29. Chernova A, et al. UPLC–MS Triglyceride Profiling in Sunflower and Rapeseed Seeds. Biomolecules. (2019) 9 (1): 9.
30. Alam S, Algahtani MS, Ahmad MZ, Ahmad J. Investigation Utilizing the HLB Concept for the Development of Moisturizing Cream and Lotion: In-Vitro Characterization and Stability Evaluation. Cosmetics. (2020) 7 (2): 43.
31. Zhuang B, Ramanauskaite G, Koa ZY, Wang ZG. Like dissolves like: A first-principles theory for predicting liquid miscibility and mixture dielectric constant. Sci. Adv. (2021) 7 (7): eabe7275.
32. Hong M. What is the Polydispersity Index (PDI) in Dynamic Light Scattering (DLS)? [Internet]. Malvern Panalytical. 2025 [cited 2025 Oct 3]. Available from: https://www.malvernpanalytical.com/en/learn/knowledge-center.
33. Farshi P, Tabibiazar M, Ghorbani M, Mohammadifar M, Amirkhiz MB, Hamishehkar H. Whey protein isolate-guar gum stabilized cumin seed oil nanoemulsion. *Food Biosci.* (2019) 28: 49–56.
34. Almadiy AA, Nenaah GE. Bioactivity and safety evaluations of Cupressus sempervirens essential oil, its nanoemulsion and main terpenes against Culex quinquefasciatus Say. *Environ. Sci. Pollut. Res.* (2022) 29 (9): 13417–13430.
35. Ali MY, et al. Nutritional Composition and Bioactive Compounds in Tomatoes and Their Impact on Human Health and Disease: A Review. Foods. (2021) 10 (1): 45.
36. Hassanpour SH, Doroudi A. Review of the antioxidant potential of flavonoids as a subgroup of polyphenols and partial substitute for synthetic antioxidants. Avicenna J. Phytomedicine. (2023) 13 (4): 354–376.
.37. Dos Santos ÉL, Siqueira JMF, Da Silva De Jesus G, Micheletti AC, Yoshida NC. Potential of Essential Oil from Siparuna guianensis A. DC. (Siparunaceae) as an Antimicrobial Adjuvant in Topical Formulations. Cosmetics. (2025) 12 (2): 81.
38. Fitriana WD, Ersam T, Shimizu K, Fatmawati S. Antioxidant Activity of Moringa oleifera Extracts. Indones. J. Chem. (2018) 16 (3): 297–301.
39. Kotíková Z, Lachman J, Hejtmánková A, Hejtmánková K. Determination of antioxidant activity and antioxidant content in tomato varieties and evaluation of mutual interactions between antioxidants. LWT - *Food Sci. Technol.* (2011) 44 (8): 1703–1710.
40. Pan Y, Li H, Zhang B, Deng Z, Shahidi F. Antioxidant interactions among hydrophilic and lipophilic dietary phytochemicals based on inhibition of low-density lipoprotein and DNA damage. J. Food Biochem. (2022) 46 (10): e14267.
41. Martin AN, Bustamante P, Chun AHC. Physical Pharmacy: Physical Chemical Principles in the Pharmaceutical Sciences. Lea & Febiger: Philadelphia (1993).
42. Islam S, Ahmed MMS, Islam MA, Hossain N, Chowdhury MA. Advances in nanoparticles in targeted drug delivery–A review. Results. Surf. Interfaces. (2025) 19: 100529.

This open-access article is distributed under the terms of the Creative Commons Attribution Non Commercial 4.0 License (CC BY-NC 4.0).

43. Gressler S, Hipfinger C, Part F, Pavlicek A, Zafiu C, Giese B. A systematic review of nanocarriers used in medicine and beyond — definition and categorization framework. J. Nanobiotechnology. (2025) 23: 90.
44. Tian L, He H, Tang X. Stability and degradation kinetics of etoposide-loaded parenteral lipid emulsion. J. Pharm. Sci. (2007) 96 (7): 1719–1728.
45. Darijani M, Shahraki M, Mostafa Habibi-Khorassani S. Theoretical study on the mechanism and kinetics of the formation β-carotene epoxides from the oxidative degradation of β-carotene. Food Chem. (2022) 389: 133082.
46. Atencio S, Verkempinck SHE, Reineke K, Hendrickx M, Van Loey A. Heat and Light Stability of Pumpkin-Based Carotenoids in a Photosensitive Food: A Carotenoid-Coloured Beverage. *Foods.* (2022) 11 (3): 485.
47. Cuvelier M-E, Soto P, Courtois F, Broyart B, Bonazzi C. Oxygen solubility measured in aqueous or oily media by a method using a non-invasive sensor. Food Control. (2017) 73: 1466–1473.
48. Ha E, Wang W, John Wang Y. Peroxide formation in polysorbate 80 and protein stability. J Pharm Sci. (2002) 91 (10): 2252–2264.
49. Yurchenko DV, et al. Catalytic Oxidation of Benzoins by Hydrogen Peroxide on Nanosized HKUST-1: Influence of Substituents on the Reaction Rates and DFT Modeling of the Reaction Path. Molecules. (2023) 28 (2): 747.
50. Ali HM, Eid SA, Eldeen HAS, Ebrahim MEH. Oxidative degradation pathways of carrot carotenes and their protection via chitosan-TPP encapsulation. *Chem. Biol. Technol. Agric.* (2025) 12 (1): 130.

This open-access article is distributed under the terms of the Creative Commons Attribution Non Commercial 4.0 License (CC BY-NC 4.0).